Asian Journal of Chemistry; Vol. 35, No. 10 (2023), 2554-2560

ASIAN JOURNAL OF CHEMISTRY

https://doi.org/10.14233/ajchem.2023.28160

Synthesis, Characterization, Molecular Docking and Biological Evaluation of 1,4-*Bis*(aryl-1*H*-1,2,3-triazole-4yl)methoxy)benzaldehyde Derivatives as Potential Anticancer Agents

N. SRAVANTHI[1], B. REVANTH[1], M. BHARGAVI[1,2] and P. SARITA RAJENDER[3,*]

[1]Molecular Modeling Laboratory, Department of Chemistry, Nizam College, Osmania University, Hyderabad-500001, India
[2]Department of Chemistry, St. Francis College for Women, Hyderabad-500016, India
[3]Department of Chemistry, University College of Engineering, Osmania University, Hyderabad-500007, India

*Corresponding author: E-mail: saritarajender@gmail.com; saritarajender@osmania.ac.in

Received: 15 February 2023; *Accepted*: 21 September 2023; *Published online*: 28 September 2023; AJC-21410

A series of novel analogues of 1,4-*bis*((aryl-1*H*-1,2,3-triazole-4-yl)methoxy)benzaldehydes were synthesized efficiently by click reaction *via* conventional method using 2,4-dipropyloxy benzaldehyde and aryl azides characterized by spectroscopic methods including ^{1}H NMR, ^{13}C NMR, mass and IR spectrometry. Comparative molecular docking studies were carried out for all the synthesized compounds (**4a-l**) using cancer therapeutics levatinib and vandetanib targeting the VEGFR2 protein's active region using the Glide tool in the Schrödinger suite. Among these, compounds **4b**, **4f** and **4h** showed better drug likeness functions than current cancer inhibitors of VEGFR2 protein. Furthermore, to determine ADME and toxicity properties, the pkCSM server and the QikProp module were used. Glide scores and binding free energy analyses were used to determine the lead molecules. Compounds **4b**, **4f** and **4h** revealed from docking exhibited potential *in vitro* cytotoxic activity against both MCF7 and HepG2 cell lines.

Keywords: Click reaction, Aryl azides, Molecular docking, Schrödinger suite, MCF7, HepG2.

INTRODUCTION

Health is a crucial component of human existence, making it one of the key areas of study and discovery in computer science [1]. In 2020, 19.3 million new cases of cancer will be diagnosed globally and close to 10 million individuals will pass away from the disease [2]. The known causes of cancer formation include prolonged sun exposure, smoking, radiation exposure, viruses, hormonal drugs and chemicals. It is crucial to identify malignancies as soon as in early stage in order to decrease cancer patient mortality [3]. One of the first-line methods for treating cancer is chemotherapy. Despite several serious efforts, today's drugs are far from perfection, with limited efficacy and a high incidence of side effects. Due to their high cost, most of these treatments are out of reach for the average person [4]. Therefore, modern medicinal chemistry needs to come out with an urgent requirement to design and develop new anticancer drugs [5].

The most fundamental parts of human life as well as many other sciences are profoundly impacted by the extraordinary frameworks known as heterocyclic compounds. The main components of commercially accessible medicines frequently contain them [6]. In environments with acidic and basic hydrolysis as well as in reductive and oxidative circumstances, 1,2,3-triazoles are very stable, according to evidence of a strong aromatic stabilization [7]. There is a large number of pharmacologically active 1,2,3-triazole compounds known of which many compounds are regular in clinical use [8]. These triazoles are one of the major structural components present in a wide range of bioactive compounds such as anticancer, anti-inflammatory, antimicrobial, antidepressant, anti-HIV, antibiotic medications, *etc*. [9-14] as shown in Fig. 1.

Inspired by the importance of heterocyclic compounds and biological applications of 1,2,3-triazoles, novel benzaldehyde based 1,2,3-triazole compounds were synthesized and characterized. Further, *in silico* molecular docking studies was carried out with the synthesized compounds at active site of VEGFR2 protein. The VEGFR2 protein is involved in multiple signal transduction pathways that control endothelial cell proliferation in hepato-cellular carcinoma and breast cancer

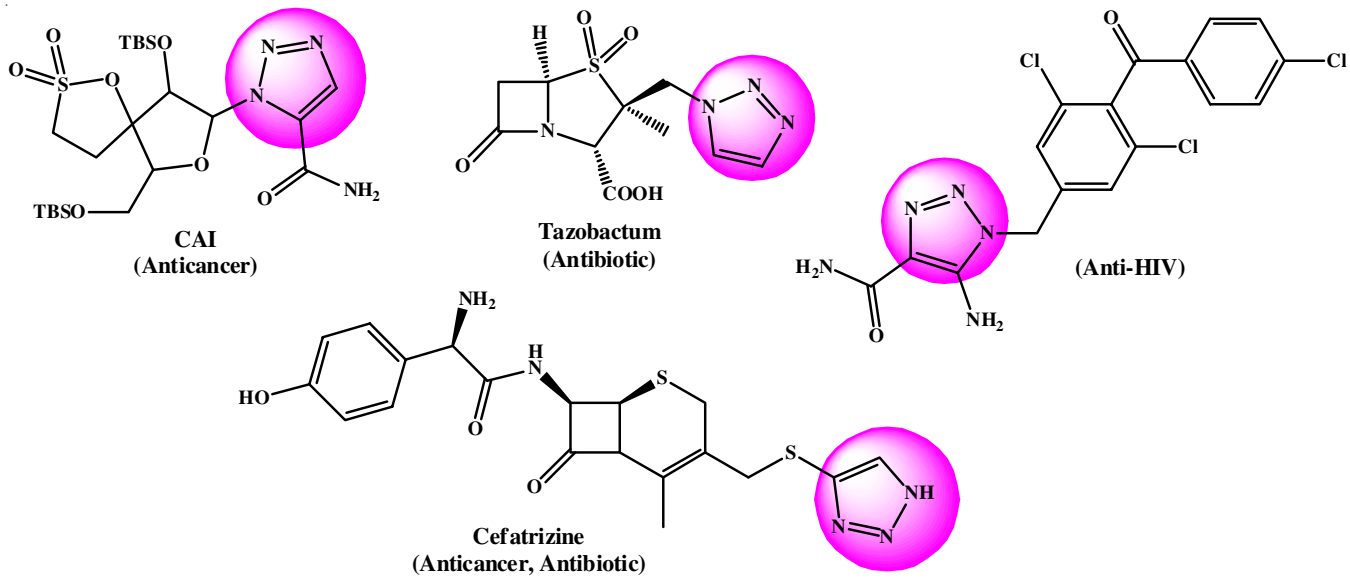

Fig. 1. Structure of some important drugs containing 1,2,3-triazole moiety

[15,16]. *In silico* studies revealed that all synthesized molecules (**4a-l**) showed better binding affinities between protein and ligand. In comparison to the already available anticancer drugs levatinib and vandetanib, compounds **4b**, **4f** and **4h** demonstrated to have effective binding affinities in terms of glide score, glide energy, binding free energies from Prime MM/GBSA and 100% human oral absorption. On the basis of assessments of cell viability and proliferation, several *in vitro* assays evaluating a cell population's reaction to external influences have been established. Using the MTT assay, best-docked molecules were evaluated for *in vitro* anticancer activity against the two different human cancer cell lines MCF-7 and HepG-2 and they exhibited activity against both cell lines.

EXPERIMENTAL

All chemicals used were of reagent grade and were not purified. A Veego melting point device was used to determine the melting points, which are uncorrected. The ^{1}H NMR spectroscopic analysis were evaluated with a Brucker AC-400F, 400 MHz spectrophotometer in $CHCl_3$-d_6 and deuterated DMSO solvents and were reported in parts per million (ppm) downfield from tetramethylsilane (Me_4Si) as an internal reference.

Synthesis of 2,4-*bis*((ethynyloxy)methyl)benzaldehyde: The reaction of 2,4-dihydroxybenzaldehyde (**1**, 1 mmol) taking place in the presence of K_2CO_3 as base dissolved in DMF. The synthesis of 2,4-*bis*((ethynyloxy)methyl)benzaldehyde was achieved after 10 to 15 min of propargyl bromide (2 mmol) being added dropwise and stirring continuously for 4 h at room temperature in an inert state (**2**). TLC was used to monitor the progress of the reaction. After the reaction was completed, the liquid was cooled to room temperature and broken ice was added before being separated with dichloromethane (3 × 40 mL). The organic layer was dried with Na_2SO_4, concentrated under vacuum and refined using a silica gel column with 20% ethyl acetate in *n*-hexane as eluent in order to obtain pure product 2,4-*bis*((ethynyloxy)methyl)benzaldehyde [17].

Synthesis of 2,4-*bis*((aryl-1*H*-1,2,3-triazol-4-yl)methoxy)benzaldehydes (4a-l): A mixture of 2,4-*bis*((ethynyloxy)-methyl)benzaldehyde (**2**, 0.92 mmol) and aryl azides (**3a-l**, 1.27 mmol) dissolved in DMF solvent were thoroughly stirred for 10-15 min. The reducing agent sodium ascorbate was added to an aqueous catalyst solution of $CuSO_4 \cdot 5H_2O$ and allowed to mix for 8-10 h. The obtained compounds **4a-l** was filtered after the reaction was completed. It was purified by crystallization and column chromatography (in solvent mixtures in specified fractions).

2,4-*Bis*((1-phenyl-1*H*-1,2,3-triazol-4-yl)methoxy)-benzaldehyde (4a): Pale white solid, yield: 78%, m.p.: 140-142 ºC. ^{1}H NMR (400 MHz, DMSO-d_6) δ ppm: 5.47 (s, 2H), 5.52 (s, 2H), 6.89 (s, 1H), 7.22 (s, 1H), 7.76-7.56 (m, 7H), 7.97 (s, 4H), 9.08 (s, 2H), 10.30 (s, 1H). ^{13}C NMR (100 MHz, DMSO-d_6) δ ppm: 61.5, 62.3, 94.5, 100.7, 108, 118.8, 122.02, 122.08, 122.6, 123.1, 129.9, 136.14, 136.17, 138.5, 138.6, 143.2, 143.7, 164.2, 164.5, 187.1. IR (neat, cm^{-1}): 1268, 1603, 1677, 2922, 3147, 3448. MS (ESI): *m/z*: 453 [M+1], $C_{25}H_{20}N_6O_3$.

2,4-*Bis*((1-(4-fluorophenyl)-1*H*-1,2,3-triazol-4-yl)-methoxy)benzaldehyde (4b): Pale white solid, yield: 80%, m.p.: 136-138 ºC. ^{1}H NMR (400 MHz, DMSO-d_6) δ ppm: 4.98 (s, 2H), 5.43 (s, 2H), 6.77-6.74 (m, 1H), 6.93-6.87 (m, 1H), 7.04-7.03 (m, 1H), 7.50-7.46 (m, 4H), 7.74-7.70 (m, 2H), 8.01-7.95 (m, 4H), 8.99 (s, 1H), 9.01 (s, 1H), 10.25 (s, 1H). ^{13}C NMR (100 MHz, DMSO-d_6) δ ppm: 187.5, 164.5, 162.1, 143.8, 143.4, 136.9, 135.3, 133.1, 129.8, 122.6, 122.5, 121.9, 121.8, 116.8, 116.6, 108.5, 100.6, 62.3, 61.5. IR (neat cm^{-1}): 1264, 1605, 1667, 2921, 3150, 3309, 3444. MS (ESI): *m/z*: 489 [M+1], $C_{25}H_{18}F_2N_6O_3$.

2,4-*Bis*((1-(2-chlorophenyl)-1*H*-1,2,3-triazol-4-yl)-methoxy)benzaldehyde (4c): Pale white solid, yield: 77%, m.p.: 132-134 ºC. ^{1}H NMR (400 MHz, DMSO-d_6) δ ppm: 5.47 (s, 1H), 5.52 (s, 2H), 6.86 (dd, *J* = 2.008 Hz, *J* = 8.78 Hz, 1H), 7.18 (d, *J* = 2.008 Hz, 1H), 7.73 (d, *J* = 8.78 Hz, 1H), 7.89-7.87 (m, 4H), 8.32-8.28 (m, 4H), 9.03 (s, 1H), 9.06 (s, 1H), 10.26 (1H). ^{13}C NMR (100 MHz, DMSO-d_6) δ ppm: 61.5, 62.3, 100.3, 108.1, 118.7, 120.1, 120.2, 122.7, 123.2, 128.7, 128.8,

129.6, 129.129.9, 136.5, 143.5, 161.9, 163.7, 164.4, 187.5. IR (neat cm^{-1}): 1254, 1666, 2928, 3132, 3442. MS (ESI) *m/z*: 521 [M+1] $C_{25}H_{18}Cl_2N_6O_3$.

2,4-*Bis*((1-(4-chlorophenyl)-1*H*-1,2,3-triazol-4-yl)-methoxy)benzaldehyde (4d): Pale white solid, yield: 82%. m.p.: 144-146 ºC. ^{1}H NMR (400 MHz, DMSO-d_6) δ ppm: 5.43 (s, 2H), 5.48 (s, 2H), 6.58-6.83 (m, 1H), 7.16 (s, 1H), 7.70-7.68 (m, 5H), 8.00-7.96 (m, 4H), 9.04 (s, 1H), 9.06 (s, 1H), 10.26 (s, 1H). ^{13}C NMR (100 MHz, DMSO-d_6) δ ppm: 61.5, 62.3, 100.6, 108.1, 116.6, 116.8, 121.8, 121.9, 122.6, 129.8, 133.1, 135.3, 143.5, 162.0, 163.7, 164.5, 187.5. IR (neat, cm^{-1}): 1261, 1603, 1676, 2923, 3147, 3421.MS (ESI): *m/z*: 521 [M+1], $C_{25}H_{18}Cl_2N_6O_3$.

2,4-*Bis*((1-(4-iodophenyl)-1*H*-1,2,3-triazol-4-yl)-methoxy)benzaldehyde (4e): Pale white solid, yield: 82%, m.p.: 118-120 ºC. ^{1}H NMR (400 MHz, DMSO-d_6) δ ppm: 5.47-5.36 (m, 4H), 7.20-6.74 (m, 2H), 7.78 -7.71 (m, 5H), 7.98-7.96 (m, 4H), 9.05 - 9.02 (m, 2H), 10.25 (s, 1H). ^{13}C NMR (100 MHz, DMSO-d_6) δ ppm: 61.5, 62.3, 94.4, 100.7, 107.9, 118.9, 122.0, 122.1, 122.6, 123.1, 130.0, 136.1, 136.2, 138.5, 138.6, 143.3, 143.7, 164.3, 164.5, 187.1. IR (neat, cm^{-1}): 1261, 1603, 1676, 2921, 3151, 3451.MS (ESI):*m/z*: 705 [M+1], $C_{25}H_{18}I_2N_6O_3$.

2,4-*Bis*((1-(4-bromophenyl)-1*H*-1,2,3-triazol-4-yl)methoxy)benzaldehyde (4f): Pale white solid, Yield: 80%, m.p.: 140-142 ºC. ^{1}H NMR (400 MHz, DMSO-d_6) δ ppm: 5.48-5.43 (m, 4H), 7.03 (s, 1H), 7.15 (s, 1H), 7.74-7.70 (m, 4H), 7.83-7.81 (m, 3H), 7.94-7.89 (m, 2H), 9.06-90.3 (m, 2H), 10.26 (s, 1H). ^{13}C NMR (100 MHz, DMSO-d_6) δ ppm: 61.5, 62.2, 100.2, 108.2, 118.7, 121.4, 121.5, 122.0, 122.1, 122.7, 123.2, 129.6, 132.7, 132.8, 135.7, 143.3, 143.7, 162.1, 163.7, 164.5, 187.5. IR (neat, cm^{-1}): 1261, 1603, 2877, 3149, 3447. MS (ESI): *m/z*: 609 [M+1], $C_{25}H_{18}Br_2N_6O_3$.

2,4-*Bis*((1-(*m*-tolyl)-1*H*-1,2,3-triazol-4-yl)methoxy)-benzaldehyde (4g): Pale white solid, Yield: 72%, m.p.: 188-120 ºC. ^{1}H NMR (400 MHz, DMSO-d_6) δ ppm: 2.39 (s, 6H), 5.48-5.43 (m, 4H), 7.03 (d, 1H), 7.15 (d, 1H), 7.16 (s, 1H), 7.78-7.71 (m, 5H), 7.98-7.96 (m, 3H), 8.96 (s, 1H), 8.99 (s, 1H), 10.25 (s, 1H). ^{13}C NMR (100 MHz, DMSO-d_6) δ ppm: 20.5, 61.5, 62.3, 100.3, 108.1, 118.7, 120.1, 120.2, 122.7, 123.2, 128.7, 128.8, 129.6, 129.8, 129.9, 136.5, 143.5, 161.9, 163.7, 164.5, 187.5. IR (cm^{-1}): 1231, 1606, 1637, 2928, 3060, 3184, 3451. MS (ESI): *m/z*: 481 [M+1], $C_{27}H_{24}N_6O_3$.

2,4-*Bis*((1-(*p*-tolyl)-1*H*-1,2,3-triazol-4-yl)methoxy)-benzaldehyde (4h): Pale white solid, yield: 84%, m.p.: 140-142 ºC. ^{1}H NMR (400 MHz, DMSO-d_6) δ ppm: 2.39 (s, 6H), 5.41 (s, 2H), 5.46 (s, 2H), 6.84 (dd, *J* = 1.75 Hz, *J* = 8.53 Hz, 1H), 7.16 (d, *J* = 2.008 Hz, 1H), 7.41 (d, *J* = 7.27 Hz, 4H), 7.71 (d, *J* =8.53 Hz, 1H), 7.82 -7.80 (m, 4H), 8.96 (s, 1H), 8.99 (s, 1H), 10.25 (s, 1H). ^{13}C NMR (100 MHz, DMSO-d_6) δ ppm: 20.53, 61.5, 62.3, 100.3, 108.1, 118.7, 119.9, 120.1, 122.6, 123.0, 129.6, 130.1, 130.2, 134.3, 138.4, 138.5, 143.0, 143.4, 162.2, 164.5, 187.5. IR (neat, cm^{-1}): 1265, 1602, 1676, 2920, 3146, 3443. MS (ESI): *m/z*: 481 [M+1], $C_{27}H_{24}N_6O_3$.

2,4-*Bis*((1-(2-methoxyphenyl)-1*H*-1,2,3-triazol-4-yl)-methoxy)benzaldehyde (4i): Pale white solid, yield: 88%, m.p.: 118-120 ºC. ^{1}H NMR (400 MHz, DMSO-d_6) δ ppm: 3.89 (s, 4H), 5.47 (s, 2H), 5.52 (s, 2H), 6.87-6.85 (m, 1H), 7.18 (m, 1H), 7.74-7.72 (m, 1H), 7.89-7.87 (m, 4H), 8.32-8.28 (m, 4H), 8.96 (s, 1H), 8.99 (s, 1H), 10.30 (s, 1H). ^{13}C NMR (100 MHz, DMSO-d_6) δ ppm: 55.5, 61.5, 62.2, 100.6, 107.9, 118.8, 119.0, 120.7, 120.8, 123.1, 123.6, 125.5, 125.6, 129.5, 129.9, 140.7, 144.1, 146.7, 161.9, 163.7, 187.6. IR (cm^{-1}): 1258, 1601, 1682, 2924, 3149, 3422. MS (ESI): *m/z*: 513 [M+1], $C_{27}H_{24}N_6O_5$.

2,4-*Bis*((1-(4-methoxyphenyl)-1*H*-1,2,3-triazol-4-yl)-methoxy)benzaldehyde (4j): Pale white solid, yield: 88%, m.p.: 130-132 ºC. ^{1}H NMR (400 MHz, DMSO-d_6) δ ppm: 3.89 (s, 6H), 5.46 (s, 2H), 5.51(s, 2H), 6.99-6.88 (m, 1H), 7.21-7.19 (m, 5H), 7.78-7.75 (m, 1H), 7.90-7.87 (m, 4H), 8.96 (s, 1H), 8.99 (s, 1H), 10.30 (s, 1H). ^{13}C NMR (100 MHz, DMSO-d_6) δ ppm: 55.5, 61.5, 62.3, 100.3, 108.1, 114.8, 118.7, 121.8, 121.9, 122.7, 123.1, 129.6, 129.8, 129.9, 142.8, 143.2, 159.3, 159.4, 162.2, 164.5, 187.5. IR (neat, cm^{-1}): 1261, 1601, 1679, 2921, 3149, 3421. MS (ESI): *m/z*: 513 [M+1], $C_{27}H_{24}N_6O_5$.

2,4-*Bis*((1-(4-nitrophenyl)-1*H*-1,2,3-triazol-4-yl)-methoxy)benzaldehyde (4k): Pale white solid, yield: 75%, m.p.: 132-134 ºC. ^{1}H NMR (400 MHz, DMSO-d_6) δ ppm: 3.52-3.41 (m, 4H), 6.76 (s, 1H), 7.16-7.03 (m, 1H), 7.74-7.71 (m, 1H), 8.29-8.27 (m, 4H), 8.49-8.47 (m, 4H), 9.22 (s, 1H), 9.24 (s, 1H), 10.27 (s, 1H). ^{13}C NMR (100 MHz, DMSO-d_6) δ ppm: 61.4, 62.3, 100.6, 107.9, 118.9, 119.0, 120.7, 120.8, 123.1, 123.6, 125.5, 125.6, 129.5, 130.0, 140.7, 144.2, 146.8, 161.9, 163.7, 187.6. IR (neat, cm^{-1}): 1259, 1601, 1673, 2921, 3269, 3446. MS (ESI): *m/z*: 543 [M+1], $C_{25}H_{18}N_8O_7$.

2,4-*Bis*((1-(3-(trifluoromethyl)phenyl)-1*H*-1,2,3-triazol-4-yl)methoxy)benzaldehyde (4l): Pale white solid, yield: 74%, m.p.: 124-126 ºC. ^{1}H NMR (400 MHz, DMSO-d_6) δ ppm: 5.47 (s, 2H), 5.52 (s, 2H), 6.87-6.85 (m, 1H), 7.18 (s, 1H), 7.72 (s, 1H), 7.89-7.87 (m, 4H), 8.32-8.28 (m, 4H), 9.20 (s, 1H), 9.22 (s,1H), 10.29 (s, 1H). ^{13}C NMR (100 MHz, DMSO-d_6) δ ppm: 61.52, 62.29, 100.23, 108.16, 116.81, 118.69, 122.16, 122.97, 123.45, 124.05, 124.87, 125.29, 129.57, 131.25, 136.94, 143.43, 143.84, 162.12, 164.47, 187.51. IR (cm^{-1}): 1263, 1601, 1675, 2922, 3124, 3446. MS (ESI): *m/z*: 589 [M+1], $C_{27}H_{18}F_6N_6O_3$.

Molecular docking: Molecular docking studies were performed for synthesized molecules in Schrödinger suite [18,19]. The RCSB Protein Data Bank was used to retrieve the VEGFR2 protein's 3D crystalline structure (PDB ID: 1Y6A) [20,21]. The 3D structure was generated in Schrödinger suite using protein preparation wizard by applying OPLS_2005 force field made suitable for docking studies. Once the protein has been refined to the RMSD threshold score of 0.30 Å, the process is finished. In molecular docking research, the protein that had been pre-processed and improved utilized as the target structure [22]. Using the Glide tool of the Schrödinger software, a three-dimensional grid box was produced in order to identify the binding cavity residues of the VEGFR2 protein from the homologous template 1Y6A [23]. The ligands were prepared using the Schrödinger suite's Ligprep module. The 2D structures of synthesized compounds (**4a-l**) were sketched in Maestro build panel then converted to 3D structures using Ligprep module and optimization was carried out with OPLS_2005 force filed [24].

The optimized protein (VEGFR2) and the ligprep out file containing synthesized compounds **4a-l** were docked using the Glide module in the Schrodinger tool in the extra precision

(XP) docking mode [25]. Prioritization of the generated novel chemical entities was done using the prime MM-GBSA with the best ADME characteristics and docking score. Using the Prime tool of the Schrödinger software and the OPLS 2005 force field, the binding free energies of receptor-ligand complexes were calculated [26,27]. The synthesized novel docked ligand molecules' pharmacokinetic characteristics were determined using the QikProp Schrödinger suite's tool [28]. The ADME parameters of all the synthesized compounds were within acceptable limits, making them new potential VEGFR2 protein inhibitors. The pkCSM server was used to identify the toxicity characteristics of the most effective medications [29].

Biological assay: The MTT assay was used to assess cell viability in three independent assays with six concentrations of substances in triplicate. The tryphan blue assay and trypsinization were used to assess the viability of the cells in suspension. In 96-well plates with 100 µL of culture media, hemocytometer-counted cells were distributed at a density of 5.0×10^3 cells per well and incubated at 37 ºC for an overnight duration. After incubation, discard the old media and replace it with 100 µL of fresh media that has a test substance in the corresponding wells of 96 plates at various concentrations. After 48 h, the drug solution was discarded and the plates were incubated for 3 h at 37 ºC with fresh medication containing MTT solution (0.5 mg/mL). After the incubation period, the MTT salt was transformed into chromophore formazan crystals by the cells with metabolically active mitochondria, resulting in precipitates. Using a microplate reader, the optical density at 570 nm of crystals that had been dissolved in DMSO was determined [30]. The percentage growth inhibition was calculated using the following formula:

$$\text{Inhibition } (\%) = \frac{(\text{Control} - \text{Treatment})}{\text{Control}} \times 100$$

A linear regression equation, $y = mx + c$, was used to calculate the IC_{50} value.

RESULTS AND DISCUSSION

The synthesis of novel 1,2,3-triazole benzaldehyde derivatives was achieved by two-steps protocol (**Scheme-I**). The first step involves 2,4-dipropyloxy benzaldehyde (**2**) by the reaction of 2,4-dihydroxybenzaldehyde (**1**) with propargyl bromide and anhydrous K_2CO_3 in DMF at room temperature. The copper-catalyzed azide-alkyne cycloaddition is one of the most well enough and simplest techniques in organic chemistry (CuAAC) [31]. Therefore, in second step, 1,2,3-triazole-based benzaldehyde compounds (**4a-l**) were exclusively obtained by condensing 2,4-dipropyloxy benzaldehyde (**2**) with various aryl azides (**3**) in the presence of $CuSO_4$ as catalyst in DMF. All compounds **4a-l** were characterized by ^{1}H NMR, ^{13}C NMR, IR and mass spectrometry.

Compound formation was proved by the disappearance and appearance of significant bands. A prominent peak for the generation of 2,4-*bis*((1-(4-fluorophenyl)-1*H*-1,2,3-triazol-4-yl)methoxy)benzaldehyde (**4b**) was visible in the IR spectra. A peak at 1254 cm^{-1} indicate C-O-C linkage, 1666 cm^{-1} indicates C=O bond, 2928 cm^{-1} indicates C-H stretching frequencies. Besides, in ^{1}H NMR spectrum, the singlet peak δ 4.98 ppm, (2H) and singlet at 5.43 ppm (2H) indicates the presence of -OCH_2 protons connecting 2 triazole rings, the singlet peak at 8.99 (1H), singlet at δ 9.08 ppm (1H) indicates the existence of two 1,2,3-triazole ring formation protons and 10.26 ppm (1H) indicates presence of an aldehyde peak remaining protons appears in the aromatic region. In ^{13}C NMR spectrum, peaks at δ 61.5 and 62.3 ppm indicate the presence of -OCH_2 carbons, 162.1 ppm, 164.5 ppm indicates the presence of 1,2,3-triazole carbons, whereas δ 164.4 ppm indicates the presence of ipso carbon attaching (oxygen attached carbons) and 187.5 ppm aldehyde carbon. Finally, the mass spectrum calculated the *m/z* at 488 and observed M+1 peak at *m/z* 489.

Molecular docking studies: The ADME characteristics of all the synthesized compounds were predicted by using Qikprop module (Table-1). These docking studies demonstrated that compounds **4b**, **4f** and **4h** protein-ligand complexes exhibited good binding affinities in Prime MM-GBSA values, good glide score and maximum human oral absorption at the active site of VEGFR2 protein (Table-2). These compounds were regularly interacted with Cys 917, Lys 918 (hydrogen bonding) and Leu 832, Val 846, Ala 864, Phe 919, Gly 920, Asn 921, Tyr 925, Lys 929, Leu 1033, Phe 1045 amino acids by (hydro-

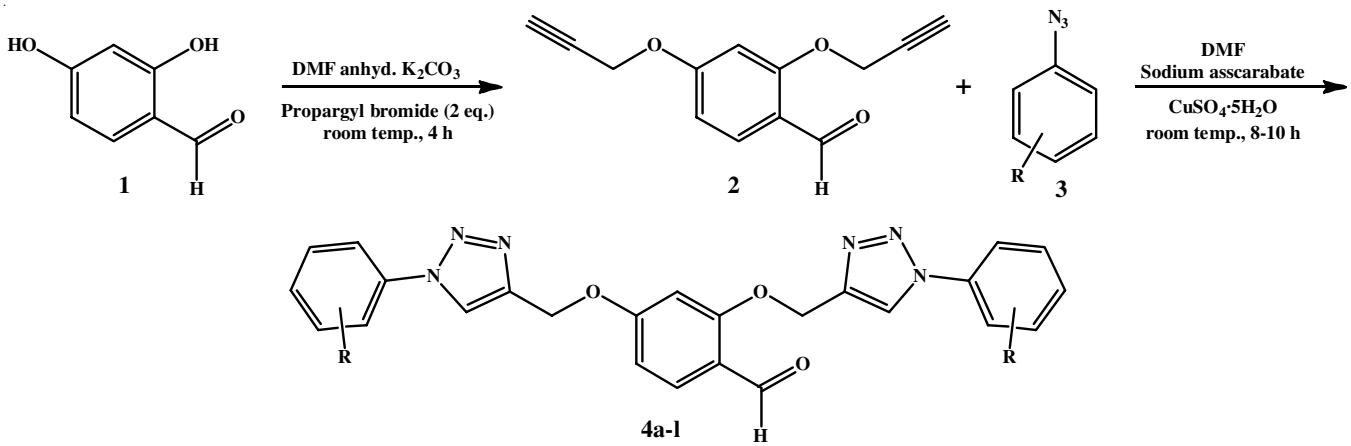

R = *p*-H, *p*-F, *o*-Cl, *p*-Cl, *p*-I, *p*-Br, *m*-Me, *p*-Me, *o*-OMe, *p*-OMe, *p*-NO_2, *m*-CF_3

Scheme-I: Synthesis of novel 1,2,3-triazole benzaldehyde analogues

TABLE-1
ADME PROPERTIES OF ALL SYNTHESIZED 12 MOLECULES FROM Qik PROP MODULE

Compound No.	m.w.	Donar HB	Accept HB	Q plog po/W	% Human oral absorption	Rule of 3	Rule of 5
4a	452	0	7.5	4.5	96	1	0
4b	487	0	7.5	5.3	100	1	2
4c	512	0	9.0	3.5	64	0	2
4d	488	0	7.5	4.4	74	1	0
4e	510	0	7.5	5.4	81	1	2
4f	492	0	7.5	5.4	74	2	2
4g	588	0	7.5	6.2	78	1	2
4h	480	0	7.5	5.1	84	1	1
4i	512	0	9.0	3.6	66	0	2
4j	542	0	9.5	2.2	25	1	2
4k	521	0	7.5	5.0	73	1	2
4l	480	0	7.5	4.7	96	1	0

TABLE-2
BEST SCORING FUNCTIONS OF SYNTHESIZED MOLECULES AND EXISTING MEDICINES AGAINST VEGFR2 PROTEIN

Compound No.	Glide score	Glide energy	% Human oral absorption	Prime MM-GBSA	Interactions (protein-ligand complex)
4b	-4.8	-49.51	100	-76.71	Hydrogen bonding: Cys 917 Hydrophobic binding: Asn 921, Gly 920, Phe1045, Leu 838, Val 846, Ala 864, Leu 1033
4f	-3.3	-52.22	81.43	-73.64	Hydrogen binding: Cys 917, Lys 918 Hydrophobic binding: Leu 838, Val 846, Ala 864, Tyr 925, Lys 929, Leu 1033, Phe 1045
4h	-5.4	-49.65	84.61	-70.09	Hydrogen binding: Cys 917 Hydrophobic binding: Leu 838, Val 846, Tyr 925
Levatinib	-4.6	-38.76	78	-65.38	Hydrogen binding: Cys 917 Hydrophobic binding: Leu 838, Val 846, Ala 864, Tyr 925, Leu 1033
Vandetanib	-4.2	-41.54	74	-69.52	Hydrophobic binding: Leu 838,, Tyr 925

phobic interaction) indicating that these residues were responsible for VEGFR2 protein inhibition as shown in Fig. 2. The pkCSM server was used to determine the toxicity characteristics of the best-hit compounds.

It confirmed that from the molecular docking studies and toxicity study, out of 12 compounds, synthesized three compounds (**4b**, **4f** and **4h**) showed good docking scores, H-bonding interactions, human oral absorption properties and less toxicity. As shown in Table-3, all the synthesized compounds had no or low toxicity profiles when compared to their more drug-like properties.

Biological assay: Compounds **4b**, **4f** and **4h** were tested for *in vitro* cytotoxicity against the human cancer cell line MCF-7 (breast), HepG2 (liver hepatocellular carcinoma cells) cell lines and the results are shown in Table-4. To determine the percentage growth inhibition, the compounds were tested using an MTT assay against breast cancer and liver cancer cell lines at various doses ranging from 100 µg/mL to 5 µg/mL. The CTC 50 values for the synthesized molecules (**4b**, **4f** and **4h**) ranged from 50.68 to 78.94 µg/mL. These compounds inhibited significantly to moderately the proliferation of cancer cells. Compound **4b**, containing 4-fluorophenyl group on the triazole ring, showed good anticancer properties with an IC_{50} value (MCF-7 = 50.68 0.927, HepG2 = 64.98 0.864) that was less active than the standard medication cisplatin. Compound **4f** with 4-bromo phenyl group (MCF-7 = 62.21 ± 0.802, HepG2

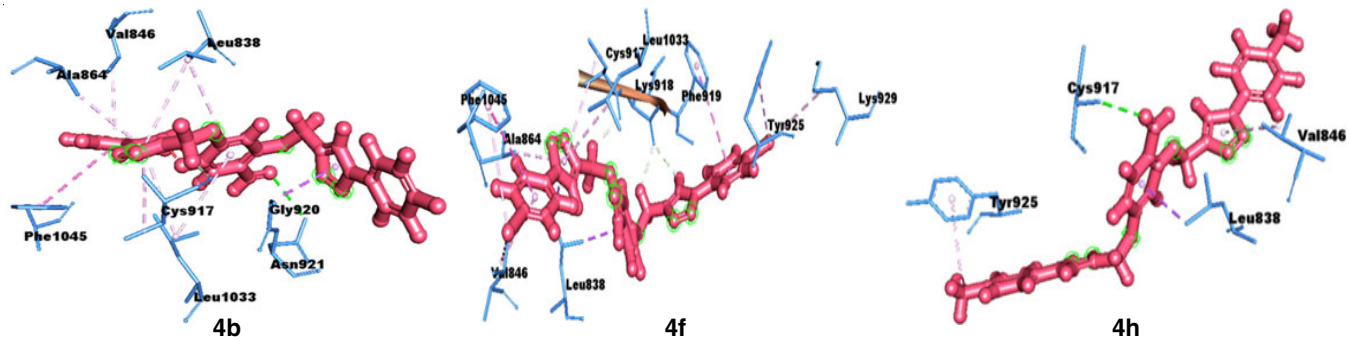

Fig. 2. Docking complexes of generated novel molecules **4b**, **4f** and **4h** were docked at the VEGFR2 protein binding site illustrated in three-dimensional structures

TABLE-3
TOXICITY PARAMETERS OF SYNTHESIZED MOLECULES **4a-l** RETRIEVED FROM THE pkCSM SERVER

Molecule	AMES toxicity	Max. tolerated dose (human)	hERG I inhibitor	hERG II inhibitor	Oral rate acute toxicity (LD_{50})	Oral rate chronic toxicity (LOAEL)	Minnow toxicity
4a	No	0.762	No	No	2.81	0.28	-1.80
4b	No	0.743	No	No	2.86	0.07	-1.81
4c	No	0.695	No	No	2.89	-0.11	-2.11
4d	No	0.68	No	No	2.87	-0.06	-3.16
4e	No	0.679	No	No	284	-0.03	-2.58
4f	No	0.682	No	No	2.84	-0.05	-2.88
4g	No	0.682	No	No	2.89	0.40	-2.17
4h	No	0.673	No	No	2.87	0.42	-2.15
4i	No	0.743	No	Yes	2.97	0.10	-1.09
4j	No	0.749	No	Yes	2.91	0.18	-2.27
4k	No	0.465	No	Yes	3.03	-0.35	-4.03
4l	No	0.685	No	Yes	2.87	-0.55	-2.17

AMES toxicity (No (no mutagenic), Oral rate acute toxicity (LD_{50}) ≥ 1000 to 5000 mg/kg, Yes (mutagenic)) Max. tolerated dose (MRTD ≥ 0.477), Minnow toxicity: log LC_{50} >– 0.3.

= 78.94 ± 0.492) and Compound **4h** with 4-methyl phenyl group (MCF-7 = 56.93 ± 0.528, HepG2 = 68.10 ± 0.492), the IC_{50} values showed slightly less anticancer activity than **4b**.

The results in Table-4 show that compounds **4b**, **4f** and **4h** exhibited potential antiproliferative effects against HepG2 and MCF7 cell lines, which are representative of liver cancer. In addition, compound **4b** demonstrated good anticancer activity against both hepatic and breast cancer cells as illustrated in Figs. 3 and 4.

Conclusion

In this study, 1,4-*bis*((aryl-1*H*-1,2,3-triazole-4-yl)methoxy)-benzaldehyde analogues (**4a-l**) were synthesized and charact-

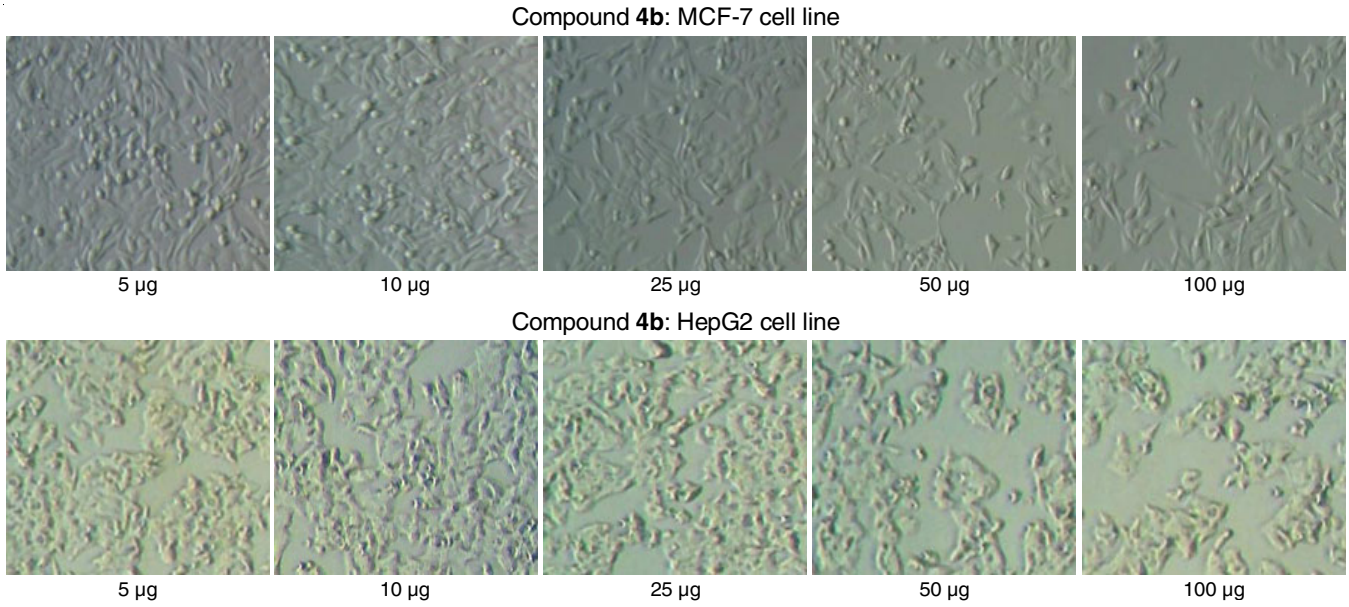

Fig. 3. Representative pictures of colonies of MCF 7 and HepG2 cell lines treated with **4b** compound

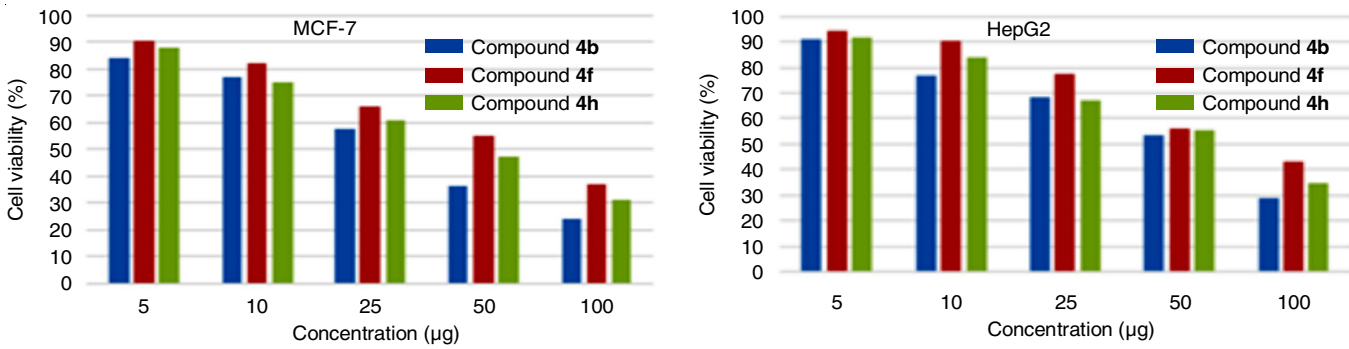

Fig. 4. Cell viability (%) of synthesized compounds (**4b**, **4f**, **4h**) against MCF7 and HepG2 cancer cell lines

TABLE-4
NOVEL COMPOUNDS' ANTIPROLIFERATIVE EFFECTS ON THE LIVER (HepG2) AND BREAST (MCF-7) CELL LINES

Compound	IC_{50} (μg)	
	MCF-7	HepG2
4b	50.68 ± 0.927	64.98 ± 0.864
4f	62.21 ± 0.802	78.94 ± 0.492
4h	56.93 ± 0.528	68.10 ± 0.492
Cisplatin (μg)	5.71 ± 0.162	12.18 ± 0.221

erized as novel and high-yielding cytotoxic scaffolds. These synthesized compounds were also docked with the VEGFR2 protein's active site. The comparitive results of the synthesized compounds' binding affinities to the therapeutic drugs levatinib and vandetanib with the VEGFR2 protein demonstrates that the synthesized compounds have effective binding interactions in terms of glidescore, glide energy, binding free energies from Prime MM/GBSA and 100% human oral absorption. The amino acid residues Cys 917, Lys 918, Leu 832, Val 846, Ala 864, Phe 919, Gly 920, Asn 921, Tyr 925, Lys 929, Leu 1033 and Phe 1045 of the VEGFR2 protein were consistently binds to synthesized compounds showing that they are crucial for the suppression of VEGFR2 protein. The most effectively docked compounds **4b**, **4f** and **4h** have *in vitro* anticancer activity against the MCF-7 and HepG2 cell lines. The cytotoxic effect of compound **4b** was greater than that of the other compounds. The overall result indicating that **4b** molecule has better glide score -4.8 kcal/mol, glide energy -49.51 kcal/mol and binding free energy -79.71 kcal/mol with 100% human oral absorption than the standard drugs levatinib and vandetanib. Thus, **4b** molecule with 1,2,3-triazole benzaldehyde scaffold seemed to be a promising candidate for the progress of new VEGFR2 inhibitors.

ACKNOWLEDGEMENTS

The authors thank The Principal and Head of the Department of Chemistry at Nizam College, Osmania University, Hyderabad, India for providing the research facilities.

CONFLICT OF INTEREST

The authors declare that there is no conflict of interests regarding the publication of this article.

REFERENCES

1. S. Nanglia, M. Ahmad, F. Ali Khan and N.Z. Jhanjhi, *Biomed. Signal Process. Control*, **72**, 103279 (2022); https://doi.org/10.1016/j.bspc.2021.103279
2. J. Ferlay, M. Colombet, I. Soerjomataram, D.M. Parkin, M. Piñeros, A. Znaor and F. Bray, *Int. J. Cancer*, **149**, 778 (2021); https://doi.org/10.1002/ijc.33588
3. F. Gouzerh, J.-M. Bessière, B. Ujvari, F. Thomas, A.M. Dujon and L. Dormont, *Biochim. Biophys. Acta Rev Cancer*, **1877**, 188644 (2022); https://doi.org/10.1016/j.bbcan.2021.188644
4. P. Bhatt, M. Kumar and A. Jha, *Mol. Divers.*, **22**, 827 (2018); https://doi.org/10.1007/s11030-018-9832-5
5. S. Bitla, A.A. Gayatri, M.R. Puchakayala, V. Kumar Bhukya, J. Vannada, R. Dhanavath, B. Kuthati, D. Kothula, S.R. Sagurthi and K.R. Atcha, *Bioorg. Med. Chem. Lett.*, **41**, 128004 (2021); https://doi.org/10.1016/j.bmcl.2021.128004
6. H. Mousavi, *Int. J. Biol. Macromol.*, **186**, 1003 (2021); https://doi.org/10.1016/j.ijbiomac.2021.06.123
7. A. Sahu, P. Sahu and R. Agrawal, *Curr. Chem. Biol.*, **14**, 71 (2020); https://doi.org/10.2174/2212796814999200807214519
8. S. Kumar, S.L. Khokra and A. Yadav, *Futur. J. Pharm. Sci.*, **7**, 106 (2021); https://doi.org/10.1186/s43094-021-00241-3
9. M.M. Alam, *Arch. Pharm.*, **355**, 2100158 (2022); https://doi.org/10.1002/ardp.202100158
10. C.-Y. Cheng, A. Haque, M.-F. Hsieh, S. Imran Hassan, M.S. Faizi, N. Dege and M.S. Khan, *Int. J. Mol. Sci.*, **21**, 3823 (2020); https://doi.org/10.3390/ijms21113823
11. K. Lal, P. Yadav, A. Kumar, A. Kumar and A.K. Paul, *Bioorg. Chem.*, **77**, 236 (2018); https://doi.org/10.1016/j.bioorg.2018.01.016
12. I. Khan, M.A. Tantray, H. Hamid, M.S. Alam, A. Kalam, F. Hussain and A. Dhulap, *Bioorg. Chem.*, **68**, 41 (2016); https://doi.org/10.1016/j.bioorg.2016.07.007
13. L.S. Feng, M.J. Zheng, F. Zhao and D. Liu, *Arch. Pharm.*, **354**, 2000163 (2021); https://doi.org/10.1002/ardp.202000163
14. B. Zhang, *Eur. J. Med. Chem.*, **168**, 357 (2019); https://doi.org/10.1016/j.ejmech.2019.02.055
15. C.-K. Chen, W.-H. Yu, T.-Y. Cheng, M.-W. Chen, C.-Y. Su, Y.-C. Yang, T.C. Kuo, M.T. Lin, Y.C. Huang, M. Hsiao, K.T. Hua, M.C. Hung and M.L. Kuo, *Sci. Rep.*, **6**, 31398 (2016); https://doi.org/10.1038/srep31398
16. Q. Zhang, S. Lu, T. Li, L. Yu, Y. Zhang, H. Zeng, X. Qian, J. Bi and Y. Lin, *J. Exp. Clin. Cancer Res.*, **38**, 173 (2019); https://doi.org/10.1186/s13046-019-1156-5
17. P. Prabhakaran, S. Kanagasabai, G. Seshan, K. Gugan, S. Usharani and P. Rajakumar, *Chem. Data Coll.*, **28**, 100427 (2020); https://doi.org/10.1016/j.cdc.2020.100427
18. K.K. Mustyala, V. Malkhed, V.R. Chittireddy and U. Vuruputuri, *Int. J. Mycobacteriol.*, **4**, 330 (2015); https://doi.org/10.1016/j.ijmyco.2015.05.013
19. M. Narasimha, B. Revanth, D. Mahender and P. Sarita Rajender, *Biointerface Res. Appl. Chem.*, **11**, 11088 (2020); https://doi.org/10.33263/BRIAC114.1108811103
20. D.S. Goodsell, C. Zardecki, L. Di Costanzo, J.M. Duarte, B.P. Hudson, I. Persikova, J. Segura, C. Shao, M. Voigt, J.D. Westbrook, J.Y. Young and S.K. Burley, *Protein Sci.*, **29**, 52 (2020); https://doi.org/10.1002/pro.3730
21. D.S. Goodsell and S.K. Burley, *Oncogene*, **39**, 6623 (2020); https://doi.org/10.1038/s41388-020-01461-2
22. P.C. Jilloju, P. Shyam, A. Sanjeev and R.R. Vedula, *J. Mol. Struct.*, **1225**, 129140 (2021); https://doi.org/10.1016/j.molstruc.2020.129140
23. Glide, version 6.1. Schrödinger, NY: New York, LLC (2016).
24. R.A. Friesner, J.L. Banks, R.B. Murphy, T.A. Halgren, J.J. Klicic, D.T. Mainz, M.P. Repasky, E.M. Knoll, M. Shelley, J.K. Perry, D.E. Shaw, P. Francis and P.S. Shenkin, *J. Med. Chem.*, **47**, 1739 (2004); https://doi.org/10.1021/jm0306430
25. G. Lanka, R. Bathula, M. Dasari, M. Bhargavi and S.R. Potlapally, *Int. J. Comput. Biol. Drug Des.*, **14**, 166 (2021); https://doi.org/10.1504/IJCBDD.2021.117183
26. E.A. Rifai, M. van Dijk, N.P. Vermeulen, A. Yanuar and D.P. Geerke, *J. Chem. Inf. Model.*, **59**, 4018 (2019); https://doi.org/10.1021/acs.jcim.9b00609
27. B. Ji, S. Liu, X. He, V.H. Man, X.-Q. Xie and J. Wang, *ACS Chem. Neurosci.*, **11**, 1139 (2020); https://doi.org/10.1021/acschemneuro.9b00696
28. QikProp, Schrodinger, NY: New York, LLC (2016).
29. D.E. Pires, T.L. Blundell and D.B. Ascher, *J. Med. Chem.*, **58**, 4066 (2015); https://doi.org/10.1021/acs.jmedchem.5b00104
30. A. Verma, K.N. Prasad, A.K. Singh, K.K. Nyati, R.K. Gupta and V.K. Paliwal, *J. Microbiol. Methods*, **81**, 175 (2010); https://doi.org/10.1016/j.mimet.2010.03.001
31. C.B. Pradeep Kumar, B.S. Prathibha, K.N.N. Prasad, M.S. Raghu, M.K. Prashanth, B.K. Jayanna, S. Chandrasekhar, H.D. Revanasiddappa, F.A. Alharthi and K.Y. Kumar, *Bioorg. Med. Chem. Lett.*, **36**, 127810 (2021); https://doi.org/10.1016/j.bmcl.2021.127810